2012

Proportional mouse model for aerosol infection by influenza

R. S. McDonald

A. R. Sambol

B. K. Heimbuch

T. L. Brown

S. H. Hinrichs

See next page for additional authors

Authors

R. S. McDonald, A. R. Sambol, B. K. Heimbuch, T. L. Brown, S. H. Hinrichs, and J. D. Wander

Journal of Applied Microbiology

Journal of Applied Microbiology ISSN 1364-5072

ORIGINAL ARTICLE

Proportional mouse model for aerosol infection by influenza

R.S. McDonald[1], A.R. Sambol[2], B.K. Heimbuch[1], T.L. Brown[2], S.H. Hinrichs[2] and J.D. Wander[3]

1 Applied Research Associates, Inc., Panama City, FL, USA
2 University of Nebraska Medical Center, 985900 Nebraska Medical Center, Omaha, NE USA
3 Airbase Sciences Branch, Air Force Research Laboratory, Tyndall AFB, FL USA

Keywords
aerosol, H1N1, infection, influenza, inhalation, mouse, respiratory protection.

Correspondence
Joseph Wander, Air Force Research Laboratory, 139 Barnes Drive, Suite 2, Tyndall AFB, FL 32403. E-mail: joseph.wander@us.af.mil

2012/0336: received 22 February 2012, revised 13 July 2012 and accepted 16 July 2012

doi:10.1111/j.1365-2672.2012.05402.x

Abstract

Aims: The aim of this study was to demonstrate a prototype tool for measuring infectivity of an aerosolized human pathogen – influenza A/PR/8/34 (H1N1) virus – using a small-animal model in the Controlled Aerosol Test System (CATS).
Methods and Results: Intranasal inoculation of nonadapted H1N1 virus into C57BL, BALB/c and CD-1 mice caused infection in all three species. Respiratory exposure of CD-1 mice to the aerosolized virus at graduated doses was accomplished in a modified rodent exposure apparatus. Weight change was recorded for 7 days postexposure, and viral populations in lung tissue homogenates were measured post mortem by DNA amplification (qRT-PCR), direct fluorescence and microscopic evaluation of cytopathic effect. Plots of weight change and of PCR cycle threshold vs delivered dose were linear to threshold doses of ~40 $TCID_{50}$ and ~12 $TCID_{50}$, respectively.
Conclusions: MID_{50} for inspired H1N1 aerosols in CD-1 mice is between 12 and 40 $TCID_{50}$; proportionality to dose of weight loss and viral populations makes the CD-1 mouse a useful model for measuring infectivity by inhalation.
Significance and Impact of the Study: In the CATS, this mouse–virus model provides the first quantitative method to evaluate the ability of respiratory protective technologies to attenuate the infectivity of an inspired pathogenic aerosol.

Introduction

Bioaerosols and transmission of respiratory diseases

Whereas aerosols and contact are accepted as modes of transmitting many disease-causing organisms, including *Legionella pneumophila*, smallpox, severe acute respiratory syndrome (SARS), coronaviruses, rhinovirus (Fiegel *et al.* 2006) and tuberculosis (Wells 1934; Riley *et al.* 1959; McClement and Christianson 1980), the role of bioaerosols as a transmission mechanism for influenza is less clearly understood (Tellier 2006; Tellier 2007a,b; Lemieux and Brankston, 2007; Brankston *et al.* 2007; Tang and Li, 2007; Lee 2007).

Although a few publications have documented the transmissibility of influenza A through inhalation routes (Tellier 2006, 2009), few studies to date have utilized a mouse model to investigate susceptibility to and pathogenicity of measured aerosol exposures. The lack of aerobiology studies results from several factors, including the need for specialized equipment to generate and monitor bioaerosols, the technical difficulty involved, inconsistency among reported techniques (Lore *et al.* 2011) and the considerable cost of conducting this research (Sherwood *et al.* 1988). Therefore, the most commonly described method of infecting mice with influenza virus is through the installation of fluid into the nasal passages (Lu *et al.* 1999; Govorkova *et al.* 2007; Gillim-Ross *et al.* 2008; Chen *et al.* 2011).

For more than 75 years, laboratory mice have served as models for susceptibility to and pathogenesis of influenza disease (Andrewes *et al.* 1934). Their low cost, small size, relative susceptibility to the virus and ease of handling make mice a favourable platform for studying influenza

virus infections. The mouse is currently considered the primary model for the evaluation of influenza antiviral agents because it is a predictive indicator of the efficacy of such treatments in humans (Sidwell and Smee 2004). The use of a well-characterized mouse model is especially important in studying the infectious pathways of new pandemic (pdm) subtypes of influenza A. Indeed, the latest emergence of influenza has reignited interest in the use of mouse models (Beigel and Bray 2008).

Although mathematical models have been used for decades (Findeisen 1935; Yeh *et al.* 1976; International Commission on Radiological Protection (ICRP) 1994; Asgharian and Anjilvel 1998; Heyder 2004) to calculate particle deposition within the respiratory tract, such calculations of particle placement are able to rationalize but not to predict the resulting clinical effect. Animal models allow closer approximation to a human response (Schulman 1968; Lowen *et al.* 2006; Gustin *et al.* 2011), and therefore, it is important to continue to further develop these models (Fouchier *et al.* 2012; Kawaoka 2012).

Experimental inhalation exposure systems are an established tool and the subject of several reviews (Drew and Laskin 1973; MacFarland 1983; Cheng and Moss 1995; Jaeger *et al.* 2006; Wong 2007). The purpose of this study was to identify and evaluate a mouse model as a complement to a measured-dose bioaerosol delivery apparatus termed CATS (Controlled Aerosol Test System) for testing the clinical effectiveness of media used in respiratory protective equipment (RPE). This validation, which includes complementary data measured postmortem, renders the mice available to serve as a detector to evaluate the clinical significance of articles of RPE by directly measuring the change in infectivity the protective article causes.

Influenza animal model

Exposure to influenza virus often leads to a disease presenting as an acute and temporarily incapacitating infection of the upper respiratory tract that can be fatal. Influenza illness is often associated with occurrences of annual or near-annual epidemics in temperate climate zones. Within the last 100 years, influenza pandemics have occurred four times [1918 (H1N1), 1957 (H2N2), 1968 (H3N2) and 2009 (H1N1)] (Oxford 2000). Pandemics are infrequent but often severe events because of the emergence of novel, unpredictable strains of influenza A virus caused by recombination of genetic material from two or more circulating virus subtypes. This antigenic shift can often lead to a new virus subtype with the ability to jump from one species into another, potentially naive species (e.g. avian influenza), and cause a large proportion of influenza-related deaths. A number of animal models have been studied to evaluate new vaccines and other approaches for preventing influenza-related disease (Gubareva *et al.* 1998; Ng *et al.* 2010). Green and Kass (1964) conducted studies on the clearance of inhaled microbial aerosols from the murine respiratory tract. Schulman and Kilbourne (1963) studied mouse-to-mouse transmissibility of influenza virus.

A factor complicating viral research in animal models is that a virus may be present in a host without causing disease. This may be due to restrictions such as the absence of appropriate receptors on certain cell types (e.g. tissue tropism) and the lack of intracellular processes required to generate infectious progeny viruses or induce cytolytic effects. Differences in viral receptors have been documented for respiratory epithelial cells based on location in either the pharynx or peripheral lung (van Riel *et al.* 2007, 2010). In addition, either the organism or host cell may mount an immune response or generate intracellular molecules that disrupt the viral effects. Therefore, differences may appear at either the cellular or tissue level or among susceptible hosts depending upon the method of infection, especially in regard to aerosol exposures (Phalen *et al.* 2008). This study examined these parameters related to efficient (near threshold) infection versus overwhelming infection of mice by exposure to aerosolized influenza virus.

Materials and methods

Exposure system description and operation

The CATS is an apparatus that was designed, constructed and validated (Stone 2010; Stone *et al.*, 2012) to deliver a precisely measured aerosol concentration, either directly or after passage through a filter medium, through a Nose-Only Directed-Flow Inhalation Exposure System (NOIES; CH Technologies, Westwood, NJ, USA, Jaeger *et al.* 2006) to individual mice (Figs 1 and 2). This low-flow, single-pass design consists of an aerosol generator, diffusion drier, charge neutralizer, filter holder, sampling points and NOIES unit (Stone 2010; Stone *et al.*, 2012). The CATS generates a biological aerosol over a range of constant concentrations and – after conditioning and treatment, if any is applied – delivers the particles to the nose of a mouse constrained in a polycarbonate tube (CHT-247; CH Technologies) as a pure respiratory exposure.

The main system components were connected using 0·5-inch (12·7-mm) stainless steel tubing with a minimum number of gradual bends. In operation, a single-jet Collison nebulizer (BGI Inc., Waltham, MA, USA), regulated to 25–30 psi was used to atomize the viral suspensions. The aerosol, which acquires surface charges during atomization, passes through a 9·5-inch (23-cm) diffusion drier and then through a 2-mCi ^{85}Kr charge neutralizer (TSI Inc., Shoreview, MN, USA) to restore the

Journal of Applied Microbiology © 2012 The Society for Applied Microbiology
113, 767–778 No claim to US Government works

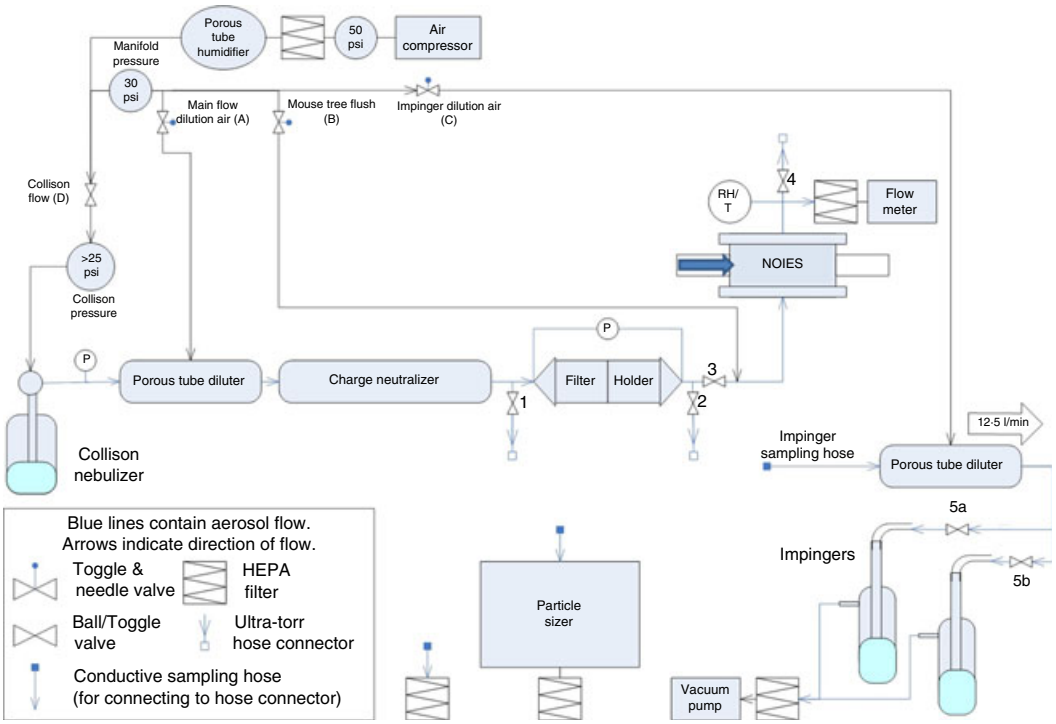

Figure 1 Schematic of the Controlled Aerosol Test System (CATS). Live virus aerosols were used to determine MID_{50} of Influenza A/PR/8/34 (H1N1) in a live animal model. Each mouse's nose (arrow) penetrates from a radially oriented constraint through the perimeter of the nose-only inhalation exposure system (NOIES).

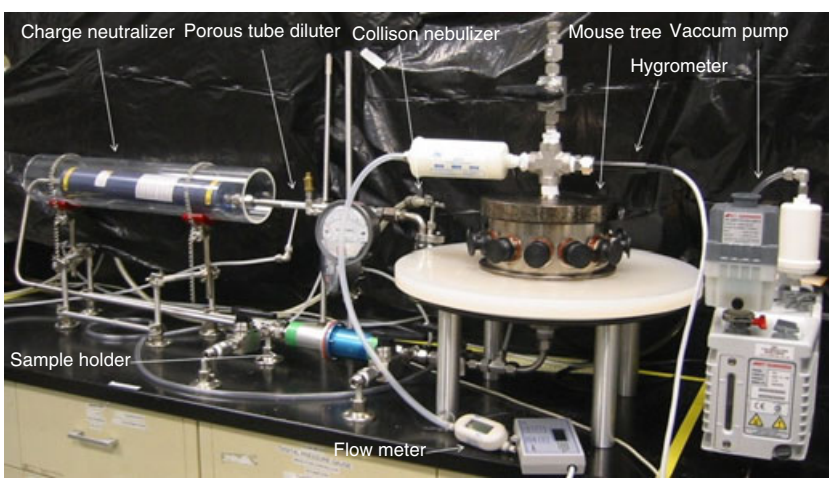

Figure 2 Photograph of Controlled Aerosol Test System (CATS), with key components labelled. Not pictured: control panel, constraints and impinger hook-up.

'normal' Boltzmann equilibrium charge distribution. After passage through the filter holder and any filter medium mounted in it, the aerosol enters the 12-port NOIES, from which it exits the test system through the HEPA-filtered exhaust. Total flow rate through the system was regulated at the nebulizer to deliver $2{\cdot}0 \pm 0{\cdot}1$ l min^{-1} measured on exit by a mass flow metre (TSI Model 4043E). The entire system was designed to fit inside a biological safety cabinet (Baker Company, Sanford, ME, USA; SG603-ATS) for additional protection from generated aerosols. The unique feature of the system is an optional filter holder (Triosyn Corp, Williston, VT,

USA), which is capable of holding filter media samples 47 mm in diameter. Smaller discs of filter media can be accommodated with the use of reducers.

Correlation of sampling ports

Stone *et al.* (2012, Stone 2010) demonstrated uniform distribution of aerosol to several ports of the CATS. Following transport and installation of the CATS in an animal biosafety level 3 (ABL3) facility at the University of Nebraska Medical Center, the exposure system was retested to verify consistency of particle counts among all 12 ports, using tap water to generate test aerosol particles. From each of the 12 exposure ports, samples of particles delivered by a single-jet Collison nebulizer were measured in triplicate using a Scanning Mobility Particle Sizer (SMPS) system (TSI Inc., Minneapolis, MN, USA). The aerosol particle size and concentration were determined using 6·0 l min^{-1} sheath air and 0·6 l min^{-1} sample air. Data outputs from the SMPS were collected by the Aerosol Instrument Manager® Software (ver. 8.1.0.0; TSI Inc., Minneapolis, MN, USA).

Propagation of virus

Influenza A/PR/8/34 (H1N1) virus was obtained from American Type Culture Collection (Rockville, MD, USA) as frozen stock (ATCC VR-1469). Virus was propagated using CDC Unit 15G.1 protocol (Szretter *et al.* 2006). Titres were performed and calculated using the Spearman–Kärber method (Armitage and Allen 1950; Finney 1964).

Particle size distribution (PSD) of influenza aerosols

To assess the PSD of aerosols containing influenza virus, samples were taken in triplicate from the sampling port located downstream from the CATS, diluted with filtered air and routed to the SMPS. Results indicated a single-mode, polydisperse aerosol in the size range 10–400 nm.

Animal husbandry/groupings

Three strains of female mice (C57BL, BALB/c and CD-1) were purchased from Charles River Laboratories (Portage Facility, MI, USA). The mice were 6–8 weeks old and ranged in weight from 18 to 30 g. Mice were randomly divided into groups assigned to specific exposure time points, and no more than five (all in a given exposure group) were housed per cage. Animals were provided rodent chow (Harlan Teklad, USA) and water *ad libitum* and maintained on a 12-h light/dark cycle. All animal work was carried out in an ABL3 facility following institutional and regulatory procedures. To minimize artefacts caused by stress during respiratory exposure sessions, mice were preconditioned daily during the week preceding their exposure sessions (NRC 2003, 2011) by insertion into a mouse restraint device (CH247; CH Technologies) for a period that did not exceed the maximum exposure time for that experiment.

Infection exposure protocols

Intranasal inoculation

To select a suitable mouse strain for infection with the influenza A/PR/8/34 (H1N1) (not mouse-adapted) strain used in this study, two inbred (BALB/c and C57BL) and one semi-outbred strain (CD-1) of 20–25 g female mice were tested for susceptibility to infection by the virus. Individual base weights were determined prior to exposure, and all mice were weighed daily at a uniform, scheduled time throughout the study. The average weights from surviving exposed mice at day 7 were compared to the averages of control mice. All mice were euthanized by day 7 postinoculation.

The inoculum, consisting of 30 μl of virus at a concentration of $4{\cdot}74 \times 10^7$ median tissue culture infectious dose ($TCID_{50}$) ml^{-1}, was placed intranasally into each mouse. The dose was divided equally and placed droplet-by-droplet by pipette into each naris of the anesthetized (ketamine/xylazine) mouse. Following the same procedure, a 1 : 10 dilution of virus stock in 1× phosphate-buffered saline (PBS) medium was used to inoculate a second set of mice of the same three strains. In all, five mice per strain per dilution were used to determine susceptibility to the virus. Three mice per strain were used as controls. Each control mouse was intranasally inoculated with 30 μl total 1 × PBS medium as previously described (Jerrells *et al.* 2007).

Aerosol exposure

In a preliminary study conducted to establish a baseline dose of virus capable of causing infection following aerosolization, the working stock of influenza virus was diluted 1 : 30 in endotoxin-free water (Sigma, St. Louis, MO, USA) and delivered into the Collison nebulizer at $1{\cdot}58 \times 10^6$ $TCID_{50}$ ml^{-1}. Four sets of three CD-1 mice were emplaced in polycarbonate restraints, installed into the NOIES with the filter holder empty, and exposed to aerosolized virus at exposure times of 2, 6, 20 and 60 min. Aliquots of the influenza working stock ($4{\cdot}74 \times 10^7$ $TCID_{50}$ ml^{-1} titre) were subsequently diluted to 1 : 300 and 1 : 1000 (v/v) in endotoxin-free water to prepare concentrations aerosolized during three successive mouse exposure series described below. The single-jet Collison nebulizer was charged and allowed to

Journal of Applied Microbiology © 2012 The Society for Applied Microbiology
113, 767–778 No claim to US Government works

run for 5 min to stabilize the system. The bypass valve directly upstream of the CATS directed the aerosol through two HEPA filters connected in series until exposure was initiated. Nonanesthetized mice were carefully immobilized in the polycarbonate tubes so that the tip of the nose projected out of an opening in the front of the holder. The tubes were then inserted securely into a port on the CATS. Once the animals were emplaced, the test aerosol was directed through the system. Vents inside the cavity of the CATS directed an airstream containing the filtered aerosol at the nares of the mouse as her only source of breathing air. Excess aerosol flow and exhaled air were continuously swept away to preclude inhalation of previously exhaled air.

A spread of delivered doses (proportional to concentration, C, $\times$ time, t) around each dilution was achieved by varying the time of exposure. The bioaerosol dose received is calculated as follows:

$$D_p(\text{presented Dose}) = \text{viral titre} \times \text{dilution factor} \times \text{VSF} \times r_a \times V_a \times t$$

Where VSF is the ratio of viable airborne counts, in $TCID_{50}$ ml^{-1}, to viable counts, in $TCID_{50}$ ml^{-1}, in the Collison reservoir, and r_a is the respiration rate per minute, and V_a is the tidal volume in ml_A (ml of air), respectively, of the CD-1 mouse. r_a and V_a are reported (Fairchild 1972) to be 261 respirations/min and 0·16 ml_A, respectively. Thus, a mouse exposed for 2 min to a 300 : 1 dilution of a suspension containing $4{\cdot}74 \times 10^7$ $TCID_{50}$ ml^{-1} of virus inhales a dose of

$$\begin{aligned} D_p &= 4{\cdot}74 \times 10^7\,\text{TCID}_{50}\,\text{ml}^{-1} \times 1/300 \\ &\quad \times 9 \times 10^{-7}\,\text{ml}\,\text{ml}_A^{-1} \times 261\,\text{resp}\,\text{min}^{-1} \\ &\quad \times 0{\cdot}16\,\text{ml}_A\,\text{resp}^{-1} \times 2\,\text{min} \\ &= 12\,\text{TCID}_{50} \end{aligned}$$

Mice were exposed in groups for each preselected time (Tables 2–4). At the end of the exposure period, the polycarbonate tubes holding the mice were removed, and the next group was inserted, until all mice for that series of experiments were exposed. When time points allowed, the mice were inserted in overlapping groups. Unused ports were sealed with the supplier's standard plugs. All exposures were carried out within a biological safety cabinet. Control mice for 1 : 30 ($1{\cdot}58 \times 10^6$ $TCID_{50}$ ml^{-1}) and 1 : 300 ($1{\cdot}58 \times 10^5$ $TCID_{50}$ ml^{-1}) exposure groups were placed in polycarbonate tubes during the testing equal to the maximum exposure time and exposed to aerosols generated from endotoxin-free water (Sigma) containing no virus. For the 1 : 1000 ($4{\cdot}74 \times 10^4$ $TCID_{50}$) exposure group, two sets of controls were used. One mouse group was exposed as earlier, while a second group was exposed to uninfected allantoic fluid processed in the same manner as from influenza-infected eggs.

Mice were observed and weighed each of 7 days post-exposure. Severely distressed mice were euthanized after the day's weighing and, following the final weighing, all surviving mice were euthanized by administration of an overdose of ketamine/xylazine by intraperitoneal injection. A necropsy was conducted and selected portions of the lungs were selected for molecular, histological or virus culture assessment. Lung tissues aseptically placed into 2·7 mL of cold BD Universal Virus Transport Medium (Becton, Dickinson and Co., Franklin Lakes, NJ, USA) were homogenized by hand using a closed ultra tissue grinder system (Fisher Scientific, Pittsburgh, PA, USA) and then stored at −80°C.

Cell culture and molecular assays

$TCID_{50}$/CPE and DFA assays

Starting viral titres were quantified by cell culture endpoint–dilution assays performed using Madin–Darby canine kidney (MDCK) cells and calculated using the Spearman–Kärber method in units of $\log_{10}$ $TCID_{50}$ ml^{-1}. Cell culture plates containing MDCK cells were grown and maintained using standard cell culture techniques.

Presence of viable virus in homogenates of murine lung tissue was qualitatively assessed by two-concentration cell culture endpoint assays performed using MDCK cells. Cell culture plates containing MDCK cells were grown and maintained using standard cell culture techniques. Aliquots (1·0 ml) of lung homogenates were plated in serial 1 : 10 dilutions (in serum-free Eagle's minimal essential medium (EMEM)) from 10^{-1} to 10^{-4} in quadruplicate on confluent cell monolayers. The samples remained in contact with the monolayer for a 1-h incubation before 1% BSA-serum-free EMEM with trypsin was added (bovine serum albumin). The plates were incubated for 5–6 days under 5% CO_2 at 37°C prior to visualization under the microscope for cytopathic effect (CPE) or fluorescent-labelled antibody evaluation. Test plates were read using a +/− system, in which + showed disruption of the monolayer and − showed that the monolayer remained confluent.

Direct fluorescent antibody assay (DFA) was used to qualitatively determine influenza infection of the MDCK cell line using the D^3 Ultra DFA Respiratory Virus Screening and ID Kit (Diagnostic Hybrids Inc., Athens, OH, USA) per manufacturer's instructions.

RNA extraction and qRT-PCR

Ribonucleic acid (RNA) was extracted from samples using the QIAamp®MinElute®Virus Spin Kit following the manufacturer's protocol (Qiagen, Valencia, CA, USA). RNA

amplification was performed using Invitrogen's Superscript III Platinum One-Step quantitative real-time polymerase chain reaction (qRT-PCR) kit (Invitrogen, Grand Island, NY, USA). The qRT-PCR assay was run on the Roche LightCycler® 480 real-time PCR System (Roche Diagnostics, Indianapolis, IN). Assay conditions and reaction volumes were used from protocols previously described by the CDC (WHO 2009). The cycle threshold (Ct) values from replicate runs were averaged for each time point and rounded to two decimal places. The recommended cut-off Ct value of 30 was used as the criterion for infection.

Histological assay

Following fixation and routine processing, tissue sections were stained with hematoxylin and eosin and reviewed under standard light microscopy. Compared to normal tissue, influenza-infected lungs showed lobular pneumonia with interbronchial inflammation. Infected lungs also showed focal chronic inflammatory cell infiltration with a few neutrophils and some interstitial thickening. Figure 3 shows the infiltrates in the infected tissue compared to uninfected tissue.

Results

Uniformity of bioaerosol distribution to test system ports

After installation in the ABL3 cabinet, a reverification of CATS performance was conducted with water. The particle counts at each port were averaged and again seen to be uniform within 10% (data not shown). A subsequent delivery of 100 mg l^{-1} sodium chloride in water showed number mean diameter ($d_{50,n}$) = 74 nm and mass mean diameter ($d_{50,m}$) = 208 nm over the range of particle diameters from 10 to 407 nm. Figure 4 plots the coefficient of variation (COV) as a function of particle size at the 12 ports for the NaCl aerosol measurements.

Intranasal exposure

Groups of five mice were inoculated intranasally with one of two doses of virus and weighed daily for a week. Per cent changes in average weights of exposed and control groups are indicated in Table 1. The nonmouse-adapted influenza virus produced obvious infection in all three strains of mice used. As no difference in gross infectivity was indicated by weight loss (Table 1), the less-expensive CD-1 mice were selected for further study.

Aerosol exposure ($1{\cdot}58 \times 10^6$ $TCID_{50}$ ml^{-1})

Two mice were used as unexposed controls. All of the mice survived to day 7, when they were euthanized and necropsied, and their lung tissue was examined by three different assays.

At all four exposure time points, mouse lung tissues gave positive results from the qRT-PCR assay, for which a positive value was defined to be ≤ 31 Ct. DFA and CPE assays on the lung tissue were also all positive

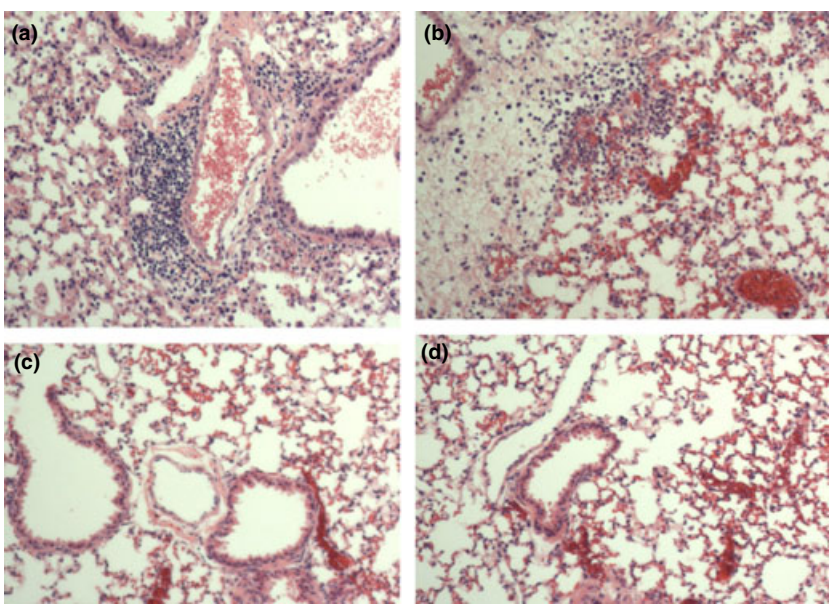

Figure 3 (a, b) Mouse lung image after exposure to aerosolized virus; H&E staining technique. (c, d) Mouse lung image after exposure to sterile aerosols (no virus noted).

Journal of Applied Microbiology © 2012 The Society for Applied Microbiology
113, 767–778

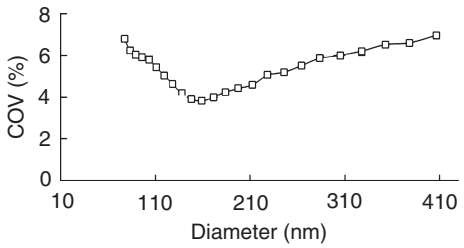

Figure 4 Size dependence in coefficient of variation of sodium chloride particle counts among ports of the CATS.

Table 1 Per cent weight loss versus controls following 30-μl intranasal inoculation of influenza virus and 7-day incubation period

	% Weight loss after intranasal inoculation (avg)		
Mouse strain	$4{\cdot}74 \times 10^7$ $TCID_{50}$ ml^{-1}	$4{\cdot}74 \times 10^6$ $TCID_{50}$ ml^{-1}	Controls
CD57BL	28·2 (SD* = 0·7)	28·0 (SD = 0·8)	0·1 (SD = 0·6)
BALB/c	26·2 (SD = 0·7)	19·0 (SD = 0·4)	0·6 (SD = 0·3)
CD-1	25·8 (SD = 0·6)	23·5 (SD = 1·5)	0·2 (SD = 0·9)

SD, standard deviation.
*One mouse died before day 7.

Table 2 Results of three assays [PCR, direct fluorescent antibody assay (DFA) and CPE] from the homogenates of CD-1 murine lung tissue exposed to an aerosol generated from $1{\cdot}58 \times 10^6$ $TCID_{50}$ ml^{-1} (1 : 30 dilution) of influenza virus over four different exposure times are indicated in parentheses: Pos = positive, Ct < 31; Neg = negative, Ct $\geq$ 37

Exposure time (min)	Presented dose ($TCID_{50}$)	Weight gain (% ±SD)*	PCR Ct	DFA	CPE
2	120	−2·0 ± 0·2	Pos (23)	Pos	Pos
6	360	−8·4 ± 0·2†	Pos (18)	Pos	Pos
20	1200	−17·3 ± 0·9	Pos (16)	Pos	Pos
60	3600	−14·7 ± 1·8	Pos (17)	Pos	Pos
Control	0	+6·9 ± 0·2	Neg (37)	Neg	Neg

*Average weight change percentage is of all three mice on day 7 postexposure.
†1/3 mice died of unrelated cause.

(Table 2). There was a direct correlation between dose received (for convenience reckoned as *Ct* values (product of concentration and exposure time)), with lower PCR Ct values resulting from prolonged exposure. The mean Ct value for control mice was 37, which was defined to be a negative response. Values of 37 > Ct > 31 were considered indeterminate. Weight losses again showed proportionality to dose delivered. The results demonstrated that the influenza virus remained viable and capable of causing infection in CD-1 mice when aerosolized under test conditions.

Aerosol exposure ($1{\cdot}58 \times 10^5$ $TCID_{50}$ ml^{-1})

Because exposure to the 1 : 30 dilution of aerosolized virus resulted in massive but graduated infection of all tested mice, a greater dilution of the working stock was delivered in an effort to identify a threshold infective dose. The dilution was increased tenfold (to 1 : 300, resulting in delivery of a $1{\cdot}58 \times 10^5$ $TCID_{50}$ ml^{-1} dispersion from the nebulizer and an overlap (as Ct products) of the two smaller doses from the 1 : 30 dilutions), and the initial aerosol exposure sequence was repeated. Three mice per time point were assayed by qRT-PCR. Variation in Ct values was observed in the 2-min exposure group, one mouse being clearly positive as reflected by Ct values, and the other two mice falling within the indeterminate range (Table 3). All mice in the 6-, 20- and 60-min time points were positive (<31 Ct) with minimal variation in Ct values. All control mice were negative (Ct values $\geq$ 37).

$TCID_{50}$ assays were performed on mice from Group 1 at each time point. One mouse lung homogenate in Group 1 that was indeterminate by qRT-PCR (36 Ct) was negative by $TCID_{50}$ assay. All other lung homogenates tested positive by both methods.

Aerosol exposure ($4{\cdot}7 \times 10^4$ $TCID_{50}$ ml^{-1})

Although weight loss by the mice appeared to have reached baseline at the dose delivered in 6 min at 1 : 300 dilution, Ct results from the aerosol challenge at 1 : 300 dilution show that all the mice exposed for 6 min or more received an infectious dose – that is, weight loss is an indicator of dose but Ct measurements provide better sensitivity to detect an endpoint. In an effort to better define the threshold at which viral infection occurs, the stock suspension was further diluted to $4{\cdot}7 \times 10^4$ $TCID_{50}$ ml^{-1} (1 : 1000), the exposure times were reduced, the number of mice per time group was increased to five, and two additional time points were added to increase the range and dose of aerosol exposure. Results of this test are shown in Table 4.

Table 3 PCR Ct values from the homogenates of CD-1 murine lung tissue exposed to bioaerosol generated from a $1{\cdot}58 \times 10^5$ $TCID_{50}$ ml^{-1} dilution of influenza virus over four different exposure times are indicated in parentheses: Pos = positive, Ct < 31; Ind = indeterminate, 37 > Ct $\geq$ 31; and Neg = negative, Ct $\geq$ 37

Exposure time (min)	Presented dose ($TCID_{50}$)	Group 1	Group 2	Group 3
2	12	Ind (36)	Pos (19)	Ind (36)
6	36	Pos (20)	Pos (21)	Pos (14)
20	120	Pos (18)	Pos (19)	Pos (20)
60	360	Pos (17)	Pos (15)	Pos (18)
Control	0	Neg	Neg	Neg

Table 4 PCR Ct values from homogenates of CD-1 murine lung tissue exposed to aerosol generated from a 4·74 × 10^4 $TCID_{50}$ ml^{-1} dilution of influenza virus over five different exposure times are indicated in parentheses: X = mouse death; Pos = positive, Ct < 31; Ind = indeterminate, 37 > Ct ≥ 31; and Neg = negative, Ct ≥ 37

Exposure time (min)	Presented dose ($TCID_{50}$)	Group 1	Group 2	Group 3	Group 4	Group 5
3	6	Neg	Neg	Neg	Neg	Neg
6	12	Neg	Neg	Neg	Neg	Pos (22)
9	18	Ind (33)	X	Neg	Ind (37)	Pos (20)
12	24	Ind (31)	Neg	Neg	Pos (23)	Neg
18	36	Ind (33)	Ind (33)	Pos (27)	Ind (37)	Neg

At the 3-min exposure time, no mice were positive for influenza virus as determined by Ct value. In all four of the longer-exposure groups, a single mouse displayed a positive *Ct* value. A trend may be suggested by the pattern of indeterminate values, but the quantitative Ct values show an equally unconvincing opposite trend. All of the lung homogenates were tested by virus cell culture assay for $TCID_{50}$ and DFA. For homogenates whose Ct value is <31, both $TCID_{50}$ and DFA were positive.

Discussion

Transmission of influenza

It is accepted that influenza may be contracted through a variety of methods including large droplet and contact transmission. The only route of infection examined during this study was inhalation of droplet nuclei through nasal passageways. Results should be expected to be different if other mucosal surfaces had been dosed with the same viral aerosols. This study sought only to determine the existence and scale of a measurable threshold aerosol infective dose in this animal model and to set parameters – such as the mouse restraints in the experiment – that limit other exposure.

Although this study demonstrated infectivity of the aerosol, its residence time as dispersed fine particles was short – hundreds of milliseconds from nozzle to nose – and viruses are known to spontaneously lose viability, so the importance of such bioaerosols as an environmental component remains uncertain. However, the experiment accurately simulates direct exposure to droplet nuclei generated by a cough, which can accordingly be concluded to be a mechanism for immediate transmission of this virus.

Animal models

The range of states resulting from influenza virus spans from asymptomatic infection to mild symptoms to pneumonia, which is often fatal. Factors such as the strain of influenza virus that caused the illness, immune status of the host and/or age of the affected individual play an important role in recovery or progression of disease. This was evident in the 2009 outbreak of influenza with the Influenza A virus H1N1 pandemic (pdm) strain, during which a disproportionately high percentage of morbidity occurred in children and young adults as well as in individuals with underlying conditions such as obesity and or diabetes (Jhung *et al.* 2011). Influenza A (H1N1) virus selected for this study was chosen based on reports of its infectivity in mice (Smee *et al.* 2008) – although it had not been mouse adapted – and its known hardiness in culture systems as a starting point for development of a mouse model for aerosolized influenza.

Infectivity/clinical symptoms

Our results showed a significant variability in morbidity and mortality among the mice exposed to aerosolized influenza virus. This appears to have been owing to individual susceptibility of the mice, because variability in the uniformity of the aerosol delivered was found not to be significant when each of the ports was analysed. In addition, significant differences were noted when mice were exposed over times ranging from 6 to 18 min with minimal or no morbidity when a low quantity of virus was sprayed over an extended period of time. Our preferred explanation is that some of the mice were able to process and clear virus, while in others, it caused clinical infection and disease. Additionally, the hardiness of immune response to influenza varies among the mice, resulting in different levels of susceptibility. For example, in Table 3 at the lowest exposure time, one of the three mice was positive for infection, whereas in the lowest dose experiment (Table 4), one mouse was positive following only 6 min of exposure.

As with many viruses, influenza produces a significant number of defective particles incapable of causing infection (Huang 1973; Pathak and Nagy 2009). This is further demonstrated by the wide variation – ranging from hundreds to thousands – in reported gene copy (total virions)-to-$TCID_{50}$ (infectious virion fraction) ratio (Yang *et al.* 2011). Sidorenko and Reichl (2004) developed a mathematical model describing the complete life cycle of influenza A in animal cells. This model, based on the multiplicity of infection (MOI) of 10 virions per cell, suggests that influenza replicates within 5 h postinfection and produces up to 8000 progeny virions before cell death occurs. Perrott *et al.* (2009) reported a detection

Journal of Applied Microbiology © 2012 The Society for Applied Microbiology
113, 767–778 No claim to US Government works

level for influenza A (H1N1) to be 1 $TCID_{50}$ for using qRT-PCR and 0·1 $TCID_{50}$ using nested qRT-PCR. Recognizing that a direct correlation may not always exist between a method that detects viable organisms and one based on viral genomes, our system showed excellent correlation between classical virology methods, morphology based on histological examination, clinical features and molecular quantification by qRT-PCR.

Influenza infection in mice has been monitored by several different parameters including mean time to death, lung weight and change in body weight (Sidwell and Smee 2000). However, these indicators are difficult to interpret when the infectivity and challenge dose of the virus does not clinically manifest an illness (morbidity or mortality). Therefore, we utilized qRT-PCR in comparison with $TCID_{50}$ to minimize the variability. Virus replication in lung tissue is considered the most informative endpoint for efficacy studies because even modest changes in virus load can have a large impact on survivability (Haga and Horimoto 2010).

Assays of postsacrifice tissue samples from the mice were uniformly positive in the 1 : 30 dilution series. In contrast with the data shown in Fig. 4, in the 1 : 300 dilution series only, the 2-min exposure (12 $TCID_{50}$ dose) group contained subjects that were not unequivocally positive for infection, both by Ct (2 of 3) and by CPE (1 of 3). One-way ANOVA and a two-tailed *t*-test did not find any statistical differences between the change in the mouse's weight and the PCR data; however, a more precise threshold value and statistical significance of this difference can be expected when the number of mice (*n*) in each exposure group is increased. Likewise, the two sets of subjects that shared *Ct* products (2 min × 1 : 30 and 20 min × 1 : 300, and 6 min × 1 : 30 and 60 min × 1 : 300) appear to show increased sensitivity with increasing aerosol concentration, which could be taken to imply that an acute exposure leads to greater infectivity than the same dose experienced more gradually. Although this interpretation is intuitively reasonable, the volume of data supporting it is too limited to justify such a conclusion.

Estimate of infective dose

Owing to logistical constraints in the ABL-3 facility, the PSD was not measured during the exposures. However, Stone *et al.* (2012; Stone 2010) measured bioaerosol particles in the range 100~500 nm for a slightly smaller virus (MS2 coli phage) in the same apparatus. The absorbed dose was likely slightly smaller than the presented dose because deposition of inspired particles in this size range is incomplete and size dependent (Stuart 1973; Clay and Clarke 1987; Heyder 2004). A plot of weight loss *vs* calculated inhaled dose (Fig. 5) was fitted to a straight line, which intersects the mean weight change of the control group at approximately 40 $TCID_{50}$. A third series of exposures was performed to a 1 : 1000 dilution, intended to improve definition of the threshold dose for weight loss; however, the results were equivocal, likely because the delivery was gradual enough that the mice developed an immune response that was able to manage the challenge, and/or the *n* of five was too small to average out what we presume to have been idiosyncrasies among the subjects.

Our results showed that qRT-PCR was more sensitive or that an excess of genome was present in comparison with the number of infectious virions as determined by $TCID_{50}$ and DFA assays. As the gold standard (Schrauwen *et al.* 2011) for determining the MOI has been $TCID_{50}$ and quantification of virus in mice exposed to influenza aerosols by qRT-PCR has not been previously reported, additional confirmatory studies were needed. We chose seven days as the terminal point for our study based on symptomatology in humans where virus production peaks approximately 48 h postinfection, and few virus particles are shed after day 6 (Taubenberger and Morens 2008). Our results showed the delivered aerosol MID_{50} to be at least 12 $TCID_{50}$ as determined by qRT-PCR Ct value and significantly <40 $TCID_{50}$ as determined by obvious clinical response. However, the sample size must be expanded in the future to achieve greater resolution and statistical significance. In addition, future studies will utilize the influenza virus A (H1N1) pdm strain to determine variation in MID_{50} between the two strains.

Future work

The data and methods presented here contribute to a fundamental basis for refining studies of aerosol delivery

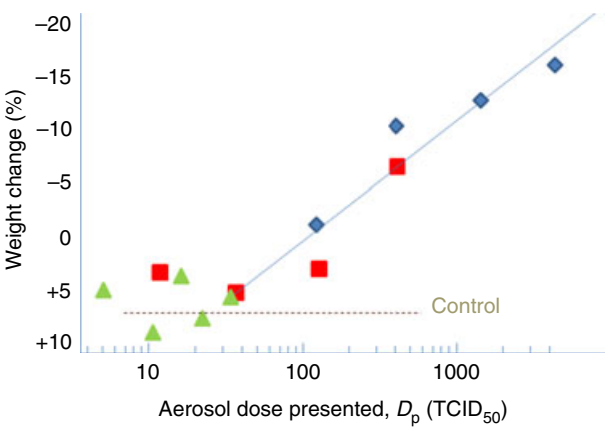

Figure 5 Average weight change for mouse exposure groups over three different received aerosol doses: ◆ = 1 : 30 dilution series; ■ = 1 : 300 dilution series; ▲ = 1 : 1000 dilution series. Plot shows overlap between doses received and change in weight, $MID_{50} \leq$ intercept of line with control value.

of particles into animal models for study of a variety of clinical subjects, such as infectious doses and vaccine delivery. Further work will be needed to more precisely define the median infective dose (MID_{50}) of the current influenza strain in the CD-1 mouse, and to better understand the effect of bioaerosol ageing and dose rate on infectivity.

Work presented herein validates aerosolization of one organism and delivery by a pure respiratory pathway into one murine host as a technique for assaying infectivity in the challenging bioaerosol. This work can serve as a starting point for a continuation of work using other microbial organisms and other animal hosts.

The intended application of the aerosol influenza animal model described here is the assessment of the clinical effect of respiratory protection devices incorporating antimicrobial treatments. Various approaches have been proposed to increase the effectiveness of respiratory filtering media including the addition of bioactive media. Although materials such as silver nanoparticles (Lala *et al.* 2007), copper oxide (Borkow *et al.* 2010), iodinated compounds (Heimbuch and Wander 2006) and others (Cecchini *et al.* 2004) have shown biocidal potential, only the iodine vector has been proposed (Lee *et al.* 2009) to operate by a noncontact mechanism. Additional studies will focus on evaluating such new technologies and, after replacement of the filter holder with a larger enclosure able to collect aerosols behind a filtering facepiece respirator (FFR) worn by an articulated headform, on quantifying the effect on protectivity of seal leakage and on optimizing the particle removal efficiency of FFRs and other RPE to maximize net protectivity.

Acknowledgements

Pilgrim's Pride Farms (Live Oak, FL) donated 100 embryonic eggs from stock-breeding hens, of which 80 were used for virus propagation and 20 served as controls. This work was supported in part by contract no. FA8650-07-C-5911, funded by the Defense Threat Reduction Agency. Protocols for animal use were approved by the University of Nebraska Medical Center Institutional Animal Care and Use Committee and all active participants received all required training prior to the acquisition of mice. Disclaimer – publication of this work does not indicate endorsement or approval of this work by the Department of Defence.

References

Andrewes, C.H., Laidlaw, P.P. and Smith, W. (1934) The susceptibility of mice to the viruses of human and swine influenza. *Lancet* **224**, 859–862.

Armitage, P. and Allen, I. (1950) Methods of estimating the LD_{50} in quantal response data. *J Hyg* **48**, 298–322.

Asgharian, B. and Anjilvel, S.A. (1998) Multiple-path model of fiber deposition in the rat lung. *Toxicol Sci* **44**, 80–86.

Beigel, J. and Bray, M. (2008) Current and future antiviral therapy of severe seasonal and avian influenza. *Antiviral Res* **78**, 91–102.

Borkow, G., Zhou, S.S., Page, T. and Gabbay, J. (2010) A novel anti-influenza copper oxide containing respiratory face mask. *PLoS ONE* **5**, e11295.

Brankston, G., Gitterman, L., Hirji, Z., Lemieux, C. and Gardam, M. (2007) Transmission of influenza A in human beings. *Lancet Infect Dis* **7**, 257–265.

Cecchini, C., Verdenelli, M.C., Orpianesi, C., Dadea, G.M. and Cresci, A. (2004) Effects of antimicrobial treatment on fiberglass–acrylic filters. *J Appl Microbiol* **97**, 371–377.

Chen, G.L., Min, J.-Y., Lamirande, E.W., Santos, C., Jin, H., Kemble, G. and Subbarao, K. (2011) Comparison of a live attenuated 2009 H1N1 vaccine with seasonal influenza vaccines against 2009 pandemic H1N1 virus infection in mice and ferrets. *J Infect Dis* **203**, 930–936.

Cheng, Y.-S. and Moss, O.R. (1995) Inhalation exposure systems. In *Concepts in Inhalation Toxicology* ed. McClellan, R.O. and Henderson, R.F. pp. 25–66. Boca Raton: CRC Press.

Clay, M.M. and Clarke, S.W. (1987) Effect of nebulised aerosol size on lung deposition in patients with mild asthma. *Thorax* **42**, 190–194.

Drew, R.T. and Laskin, S. (1973) Environmental inhalation chambers. In *Methods of Animal Experimentation*, Vol. 4 ed. Gay, W.I., pp. 1–41. New York: Academic Press.

Fairchild, G. (1972) Measurement of respiratory volume for virus retention studies in mice. *Appl Microbiol* **24**, 812–818.

Fiegel, J., Clarke, R. and Edwards, D.A. (2006) Airborne infectious disease and the suppression of pulmonary bioaerosols. *Drug Discov Today* **11**, 51–57.

Findeisen, W. (1935) Über das Absetzen kleiner, in der Luft suspendierten Teilchen in der menschlichen Lunge bei der Atmung. *Arch Ges Physiol* **236**, 367–379.

Finney, D.J. (1964) *Statistical Methods in Biological Assay*, 2nd edn. pp. 524–530. London: Griffin.

Fouchier, R.A., García-Sastre, A., Kawaoka, Y., Barclay, W.S., Bouvier, N.M., Brown, I.H., Capua, I., Chen, H. *et al.* (2012) Pause on avian flu transmission research (letter). *Science* **335**, 400–401.

Gillim-Ross, L., Santos, C., Chen, Z., Aspelund, A., Yang, C.F., Ye, D., Jin, H., Kemble, G. *et al.* (2008) Avian influenza H6 viruses productively infect and cause illness in mice and ferrets. *J Virol* **82**, 10854–10863.

Govorkova, E.A., Ilyushina, N.A., Boltz, D.A., Douglas, A., Yilmaz, N. and Webster, R.G. (2007) Efficacy of oseltamivir therapy in ferrets inoculated with different clades of H5N1 influenza virus. *Antimicrob Agents Chemother* **51**, 1414–1424.

Green, G.M. and Kass, E.H. (1964) Factors influencing the clearance of bacteria by the lung. *J Clin Invest* **43**, 769–776.

Gubareva, L.V., McCullers, J.A., Bethell, R.C. and Webster, R. G. (1998) Characterization of influenza A/HongKong/156/97 (H5N1) virus in a mouse model and protective effect of Zanamivir on H5N1 infection in mice. *J Infect Dis* **178**, 1592–1596.

Gustin, K.M., Belser, J.A., Wadford, D.A., Pearce, M.B., Katz, J.M., Tumpey, T.M. and Maines, T.R. (2011) Influenza virus aerosol exposure and analytical system for ferrets. *Proc Natl Acad Sci USA* **108**, 8432–8437.

Haga, T. and Horimoto, T. (2010) Animal models to study influenza virus pathogenesis and control. *Open Antimicrob Agents J* **2**, 15–21.

Heimbuch, B. and Wander, J. (2006) Bioaerosol Challenges to Antimicrobial Surface Treatments: Enchanced Efficacy Against MS2 Coli Phage of Air Filter Media Coated with Polystyrene-4-Methyltrimethylammonium Triiodide. Technical paper AFRL-ML-TY-TP-2006-4527, Tyndall AFB, FL, Air Force Research Laboratories DTIC Report number A909444.

Heyder, J. (2004) Deposition of inhaled in the human respiratory tract and consequences for regional targeting in respiratory drug delivery. *Proc Am Thorac Soc* **1**, 315–320.

Huang, A.S. (1973) Defective interfering viruses. *Annu Rev Microbiol* **27**, 101–118.

International Commission on Radiological Protection (ICRP). (1994) Human respiratory tract models for radiological protection. *Ann ICRP* **24**, 1–3.

Jaeger, R.J., Shami, S.G. and Tsenova, L. (2006) Directed-flow aerosol inhalation exposure systems: applications to pathogens and highly toxic agents. In *Inhalation Toxicology* ed. Salem, H. and Katz, S.A. pp. 73–90. Boca Raton: CRC Press.

Jerrells, T.R., Pavlik, J.A., DeVasure, J., Vidlak, D., Costello, A., Strachota, J.M. and Wyatt, T.A. (2007) Association of chronic alcohol consumption and increased susceptibility to and pathogenic effects of pulmonary infection with respiratory syncytial virus in mice. *Alcohol* **41**, 357–369.

Jhung, M.A., Swerdlow, D., Olsen, S.J., Jernigan, D., Biggerstaff, M., Kamimoto, L., Kniss, K., Reed, C. *et al.* (2011) Epidemiology of 2009 pandemic influenza A (H1N1) in the United States. *Clin Infect Dis* **52**(Suppl. 1), S13–S26.

Kawaoka, H. (2012) H5N1: Flu transmission work is urgent. *Nature* **482**, 155; doi: 10.1038/nature10884.

Lala, N.L., Ramaseshan, R., Bojun, L., Sundarrajan, S., Barhate, R.S., Ying-Jun, L. and Ramakrishna, S. (2007) Fabrication of nanofibers with antimicrobial functionality used as filters: protection against bacterial contaminants. *Biotechnol Bioeng* **97**, 1357–1365.

Lee, V. (2007) Reflection and reaction—transmission of influenza A in human beings. *Lancet Infect Dis* **7**, 760–761.

Lee, J.H., Wu, C.-Y., Lee, C.N., Anwar, D., Wysocki, K.M., Lundgren, D.A., Farrah, S., Wander, J. *et al.* (2009) Assessment of iodine-treated filter media for removal and inactivation of MS2 bacteriophage aerosols. *J Appl Microbiol* **107**, 1912–1923.

Lemieux, C. and Brankston, G. (2007) Questioning aerosol transmission of influenza. *Emerging Infect Dis* **13**, 173–174.

Lore, M.B., Sambol, A.R., Japuntich, D.A., Franklin, L.M. and Hinrichs, S.H. (2011) Inter-laboratory performance between two nanoparticle air filtration systems using scanning mobility particle analyzers. *J Nanopart Res* **13**, 1581–1591.

Lowen, A.C., Mubareka, S., Tumpey, T.M., García-Sastre, A. and Palese, P. (2006) The guinea pig as a transmission model for human influenza viruses. *Proc Natl Acad Sci USA* **103**, 9988–9992.

Lu, X., Tumpey, T.M., Morken, T., Zaki, S.R., Cox, N.J. and Katz, J.M. (1999) A mouse model for the evaluation of pathogenesis and immunity to influenza A (H5N1) viruses isolated from humans. *J Virol* **73**, 5903–5911.

MacFarland, H.N. (1983) Designs and operational characteristics of inhalation exposure equipment — a review. *Fund Appl Toxicol* **3**, 603–613.

McClement, J.H. and Christianson, L.C. (1980) Clinical forms of TB. In *Pulmonary Diseases and Disorders*, ed. Fishman, A.P.. pp. 1288. New York: McGraw–Hill.

Ng, W.C., Wong, V., Muller, B., Rawlin, G. and Brown, L.E. (2010) Prevention and treatment of influenza with hyperimmune bovine colostrum antibody. *PLoS ONE* **5**, e13622. doi:10.1371/journal.pone.0013622.

NRC (2003) *Guidelines for the Care and Use of Mammals in Neuroscience and Behavioral Research*, pp 48–49. Washington, DC: The National Academies Press.

NRC (2011) *Guide for the Care and Use of Laboratory animals*, 8th edn, pp. 29–30. Washington, DC: The National Academies Press.

Oxford, J.S. (2000) Influenza A pandemics of the 20th century with special reference to 1918: virology, pathology and epidemiology. *Rev Med Virol* **10**, 119–133.

Pathak, K. and Nagy, P. (2009) Defective interfering RNAs: foes of viruses and friends of virologists. *Viruses* **1**, 895–919.

Perrott, P., Smith, G., Ristovski, Z., Harding, R. and Hargreaves, M.A. (2009) Nested real-time PCR assay has an increased sensitivity suitable for detection of viruses in aerosol studies. *J Appl Microbiol* **106**, 1438–1447.

Phalen, R.F., Oldham, M.J. and Wolff, R.K. (2008) The relevance of animal models for aerosol studies. *J Aerosol Med Pulm Drug Deliv* **21**, 113–124.

van Riel, D., Munster, V.J., Leijten, L.M., Chutinimitkul, S., Munster, V.J., de Wit, E., Rimmelzwaan, G.F., Fouchier, R. A. *et al.* (2007) Human and avian influenza viruses target different cells in the lower respiratory tract of humans and other mammals. *Am J Pathol* **171**, 1215–1223.

van Riel, D., den Bakker, M.A., Leijten, L.M., Chutinimitkul, S., Munster, V.J., de Wit, E., Rimmelzwaan, G.F., Fouchier, R.A. *et al.* (2010) Seasonal and pandemic human influenza viruses attach better to human upper respiratory tract epithelium than avian influenza viruses. *Am J Pathol* **176**, 1614–1618.

Riley, R.L., Mills, C.C., Nyka, W., Weinstock, N., Storey, P.B., Sultan, L.U., Riley, M.C. and Wells, W.F. (1959) Aerial dissemination of pulmonary tuberculosis. A two-year study of contagion in a tuberculosis ward. *Am J Hyg* **70**, 185–196. reprinted in *Am J Epidemiol* **142**, 3–14 (1995).

Schrauwen, E.J.A., Herfst, S., Chutinimitkul, S., Bestebroer, T. M., Rimmelzwaan, G.F., Osterhaus, A.D.M.E., Kuiken, T. and Fouchier, R.A.M. (2011) Possible increased pathogenicity of pandemic (H1N1) 2009 influenza virus upon reassortment. *Emerg Infect Dis* **17**, 200–208.

Schulman, J.L. (1968) The use of an animal model to study transmission of influenza virus infection. *Am J Public Health Nations Health* **58**, 2092–2096.

Schulman, J.L. and Kilbourne, E.D. (1963) Experimental transmission of influenza virus infection in mice. I. The period of transmissibility. *J Exp Med* **118**, 257–266.

Sherwood, R.L., Thomas, P.T., Kawanishi, C.Y. and Fenters, J.D. (1988) Comparison of *Streptococcus zooepidemicus* and influenza virus pathogenicity in mice by three pulmonary exposure routes. *Appl Environ Microbiol* **54**, 1744–1751.

Sidorenko, Y. and Reichl, U. (2004) Structured model of influenza virus replication in MDCK cells. *Biotechnol Bioeng* **88**, 1–14.

Sidwell, R.W. and Smee, D.F. (2000) In vitro and in vivo assay systems for study of influenza virus inhibitors. *Antiviral Res* **48**, 1–16.

Sidwell, R.W. and Smee, D.F. (2004) Experimental disease models of influenza virus infections: recent developments. *Drug Discov Today Dis Models* **1**, 57–63.

Smee, D.F., Bailey, K.W., Wong, M.-H., O'Keefe, B.R., Gustafson, K.R., Mishin, V.P. and Gubareva, L.V. (2008) Treatment of influenza A (H1N1) virus infections in mice and ferrets with cyanovirin-N. *Antiviral Res* **80**, 266–271.

Stone, B.R. (2010) Consistency and reproducibility of bioaerosol delivery for infectivity studies on mice. Thesis, University of Florida.

Stone, B.R., Heimbuch, B.H., Wu, C.-Y. and Wander, J.D. (2012) Design, construction and validation of a nose-only inhalation exposure system to measure infectivity of filtered bioaerosols in mice. *J Appl Micro*, in press.

Stuart, B.O. (1973) Deposition of inhaled aerosols. *Arch Intern Med* **131**, 60–73.

Szretter, K.J., Balish, A.L. and Katz, J.M. (2006) *Current Protocols in Microbiology; Unit 15G.1 Influenza: Propagation, Quantification, and Storage*. Chichester, UK: John Wiley & Sons.

Tang, J. and Li, Y. (2007) Reflection and reaction—transmission of influenza A in human beings. *Lancet Infect Dis* **7**, 758.

Taubenberger, J.K. and Morens, D.M. (2008) The pathology of influenza virus infections. *Annu Rev Pathol* **3**, 499–522.

Tellier, R. (2006) Review of aerosol transmission of influenza A virus. *Emerg Infect Dis* **12**, 1657–1662.

Tellier, R. (2007a) Questioning aerosol transmission of influenza: in response. *Emerging Infect Dis* **13**, 174–175.

Tellier, R. (2007b) Reflection and reaction— transmission of influenza A in human beings. *Lancet Infect Dis* **7**, 759–760.

Tellier, R. (2009) Aerosol transmission of influenza A virus: a review of new studies. *J R Soc Interface* **6**(Suppl. 6), S783–S790.

Wells, W.F. (1934) On air-borne infection. Study II. Droplets and droplet nuclei. *Am J Hyg* **20**, 611–618.

(WHO) World Health Organization Collaborating Centre for Influenza (2009) "CDC protocol of realtime RTPCR for influenza A(H1N1) revision 2 (6 October 2009)", p. 5, http://www.who.int/csr/resources/publications/swineflu/CDCRealtimeRTPCR_SwineH1Assay-2009_20090430.pdf

Wong, B.A. (2007) Inhalation exposure systems: design, methods, and operation. *Toxicol Path* **35**, 3–14.

Yang, W., Elankumaran, S. and Marr, L.C. (2011) Concentrations and size distributions of airborne influenza A viruses measured indoors at a health centre, a day-care centre and on aeroplanes. *J R Soc Interface* **8**, 1176–1184.

Yeh, H.C., Phalen, R.F. and Raabe, O.G. (1976) Factors influencing the deposition of inhaled particles. *Environ Health Perspect* **15**, 147–156.